

Alzheimer's disease-like pathological features in transgenic mice expressing the APP intracellular domain

Kaushik Ghosal^{a,1}, Daniel L. Vogt^{a,1}, Man Liang^a, Yong Shen^b, Bruce T. Lamb^a, and Sanjay W. Pimplikar^{a,2}

^aDepartment of Neurosciences, Lerner Research Institute, Cleveland Clinic, Mail Code NC30, 9500 Euclid Avenue, Cleveland, OH 44195; and ^bHaldeman Laboratory of Molecular and Cellular Neurobiology, Sun Health Research Institute, 10515 West Santa Fe Drive, Sun City, AZ 85351

Edited by Thomas C. Südhof, Stanford University School of Medicine, Palo Alto, CA, and approved September 11, 2009 (received for review July 20, 2009)

The hypothesis that amyloid- β ($A\beta$) peptides are the primary cause of Alzheimer's disease (AD) remains the best supported theory of AD pathogenesis. Yet, many observations are inconsistent with the hypothesis. $A\beta$ peptides are generated when amyloid precursor protein (APP) is cleaved by presenilins, a process that also produces APP intracellular domain (AICD). We previously generated AICD-overexpressing transgenic mice that showed abnormal activation of GSK-3 β , a pathological feature of AD. We now report that these mice exhibit additional AD-like characteristics, including hyperphosphorylation and aggregation of tau, neurodegeneration and working memory deficits that are prevented by treatment with lithium, a GSK-3 β inhibitor. Consistent with its potential role in AD pathogenesis, we find AICD levels to be elevated in brains from AD patients. The in vivo findings that AICD can contribute to AD pathology independently of $A\beta$ have important therapeutic implications and may explain some observations that are discordant with the amyloid hypothesis.

amyloid precursor protein | neurodegeneration | tau hyperphosphorylation

Alzheimer's disease (AD) is a neurodegenerative disorder that begins with deficits in short-term memory and culminates in total loss of cognition and executive functions. Neuropathologically, the disease is characterized by the presence of extracellular plaques enriched in amyloid-beta ($A\beta$) peptides and intracellular neurofibrillary tangles containing hyperphosphorylated tau protein (1, 2). The $A\beta$ peptides are produced by the proteolytic processing of amyloid precursor protein (APP) (3, 4), which is cleaved by 'secretases' to produce multiple fragments. According to the amyloid hypothesis, $A\beta$ peptides are the primary causative agents of AD, (5, 6), and $A\beta$ peptides have remained the focus of the vast majority of studies in this research area.

However, it is becoming clear that the $A\beta$ plaques or increased $A\beta$ load per se are unlikely to be the sole cause of AD, because a significant proportion of people without dementia have $A\beta$ deposits and clearance of $A\beta$ plaques by active immunization produced no clinical benefits (7). Also, the loss of synapses and the presence of phospho-tau in tangles seem to be better correlated with disease severity than $A\beta$ load (8). Moreover, the neurological deficits can be dissociated from $A\beta$ load in several mouse models of AD (9, 10) as well as human AD (7) and the clinical drug trials aimed at reducing $A\beta$ load (flurbiprofen) or its aggregation (tramiprosate) have yielded disappointing results. Although many factors could have influenced the failed drug trials and could be responsible for the discordant results in animal studies, the combined weight of these findings suggests that factors independent of $A\beta$ also contribute to AD pathogenesis (11, 12). Recently, soluble aggregates of $A\beta$ peptides have been proposed to be the toxic agent (13). However, the molecular nature of such soluble aggregates is uncertain and their existence and precise composition remains debated (14, 15).

The presenilin-mediated cleavage of APP that generates $A\beta$ peptides simultaneously releases APP intracellular domain

(AICD) in the cytoplasm (16). AICD has received little investigative attention relative to $A\beta$, but recent studies have begun to establish its biological significance. We and the Südhof group were first to show that free, soluble AICD enters the nucleus and alters gene transcription (17, 18). Subsequently, other studies showed that AICD alters intracellular signaling and regulates gene expression in vitro (19, 20). To study its in vivo role, we generated AICD-overexpressing mice (21) and observed activation of glycogen synthase kinase-3 β (GSK-3 β) and phosphorylation of CRMP-2 in the transgenic mice. Since both abnormalities are observed in human AD brains (22), our findings provided the clues that AICD, in addition to $A\beta$, could contribute to AD pathology.

We now provide further evidence that elevated levels of AICD in vivo cause hyperphosphorylation and age-dependent aggregation of tau and neurodegeneration without altering APP metabolism or increasing the $A\beta$ levels. In addition, the AICD transgenic mice showed deficits in working memory that were blocked by lithium treatment. Finally, we demonstrate that AICD levels are elevated in human AD brains. Our results show that AICD may play a critical role in AD pathogenesis.

Results

AICD Transgenic (FeC γ 25) Mice. The details of AICD transgenic mice generation were previously published (21). Briefly, we inserted DNA expressing the 59-residue long AICD peptide (a product of γ -cleavage), or myc-tagged Fe65 downstream of a CaMKII α promoter and co-injected the plasmid DNA into oocytes of C57BL/6 mice. We obtained several lines that co-expressed AICD and Fe65 and one line that expressed Fe65 alone (termed Fe27). Here, we studied bigenic line FeC γ 25 that expressed 1.5–2-fold higher levels of AICD in the membrane and nuclear fractions (21) compared to wild-type C57BL/6 mice. Similarly, Fe27 mice expressed approx. 1.5-fold higher levels of Fe65.

Hyperphosphorylation and Age-Dependent Aggregation of Tau in FeC γ 25 Mice. We previously observed that at 2 months of age, FeC γ 25 mice showed increased activation of GSK-3 β and phosphorylation of CRMP2 compared to Fe27 or the non-transgenic littermates (21). Aberrant activation of GSK-3 β is a key event in AD pathogenesis and contributes to hyperphosphorylation of tau. Here we used 4- and 8-month-old mice to determine the levels of phospho-tau by Western blot analysis (Fig. 1) and immunohisto-

Author contributions: K.G., D.L.V., M.L., and S.W.P. designed research; K.G., D.L.V., and M.L. performed research; Y.S. and B.T.L. contributed new reagents/analytic tools; K.G., D.L.V., and S.W.P. analyzed data; and K.G., D.L.V., and S.W.P. wrote the paper.

The authors declare no conflict of interest.

This article is a PNAS Direct Submission.

Freely available online through the PNAS open access option.

¹K.G. and D.L.V. contributed equally to this work.

²To whom correspondence should be addressed. E-mail: pimplis@ccf.org.

This article contains supporting information online at www.pnas.org/cgi/content/full/0907652106/DCSupplemental.

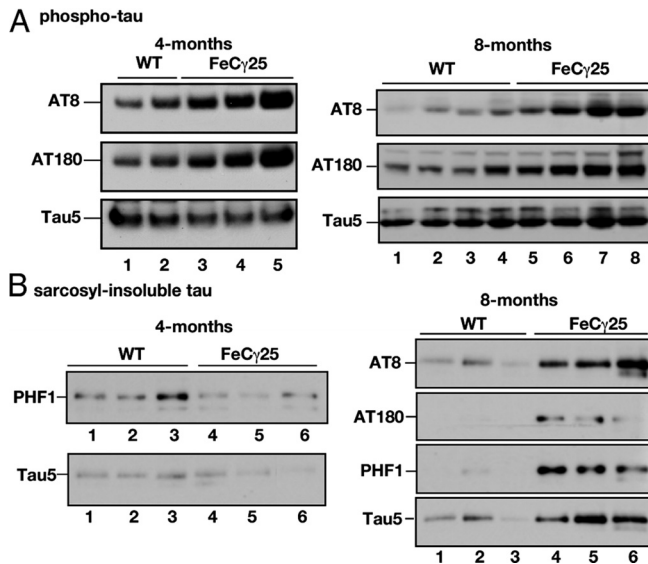


Fig. 1. Increased phosphorylation and age-dependent aggregation of tau in FeC γ 25 mice. (A) Left panel: Hippocampal brain lysates from 4-month-old wild-type mice (lanes 1, 2) or FeC γ 25 transgenic mice (lanes 3–5) were separated by SDS/PAGE and Western blotted using AT-8 (top row), AT-180 (middle row), or Tau5 (lower row) to detect phospho-tau and total tau, respectively. Note the elevated levels of phospho-tau in FeC γ 25 mice compared to wild-type controls. In contrast, total tau levels were unaltered. Right panel: Hippocampal brain lysates from 8-month-old wild-type mice (lanes 1–4) or FeC γ 25 transgenic mice (lanes 5–8) were separated by SDS/PAGE and Western blotted using AT-8 or AT-180 antibodies as described above. The phospho-tau levels remained elevated at 8 months of age in FeC γ 25 mice while the total tau levels remained essentially unchanged. (B) Left panel: Lysates from brain cortices from wild-type (lanes 1–3) or FeC γ 25 (lanes 4–6) mice were subjected to a sarcosyl extraction protocol and the detergent-insoluble fractions were Western blotted using PHF1 or Tau5 antibodies. There were no consistent differences in the amounts of detergent-insoluble tau at 4 months of age between FeC γ 25 and control mice. Right panel: Cortical brain lysates from 8-month-old wild-type (lanes 1–3) or FeC γ 25 (lanes 4–6) mice were subjected to a sarcosyl extraction protocol and the detergent insoluble fractions were Western blotted using indicated antibodies. Note the increased amounts of both phospho-tau and total tau in the sarcosyl-insoluble fraction of FeC γ 25 mice. Each lane represents an individual mouse.

chemistry (Figs. 2 and 3). We separated hippocampus and cortex from mice 3–4 months of age (Fig. 1A and B; left panels) or 7–8 months of age (Fig. 1A and B; right panels). Hippocampal lysates from multiple animals were separated by SDS/PAGE, transferred onto nitrocellulose membranes and probed with AT-8 (which detects phosphorylation at Ser-202 and Thr-205) or AT-180 (detecting phospho-Thr-231) antibodies. FeC γ 25 mice showed increased levels of both AT-8 and AT-180 immunoreactive-tau compared to non-transgenic control animals (Fig. 1A, left panel). In contrast, the amount of total tau (probed with Tau5 antibody) was not altered. Phospho-tau levels were also elevated in hippocampal lysates from multiple 8-month-old mice (Fig. 1A, right panel), whereas the total tau levels were not significantly altered (bottom row). Elevated phospho-tau levels were also observed in 12-month-old animals (Fig. S1).

To determine whether increased phosphorylation caused tau to aggregate, we subjected the cortical lysates from 4-month-old mice (Fig. 1B, left panel) or 8-month-old mice (Fig. 1B, right panel) to a sarcosyl extraction protocol (23) and determined the levels of the aggregated tau (detergent-insoluble) by Western blotting. The levels of the sarcosyl-insoluble tau in 4-month-old FeC γ 25 mice showed some variation but were not significantly different from those in control mice (Fig. 1B, left panel) when detected by PHF1 antibody (which detects pSer396, pSer 404) or Tau5. In contrast, at 8 months of age (Fig. 1B, right panel) AICD transgenic mice (lanes

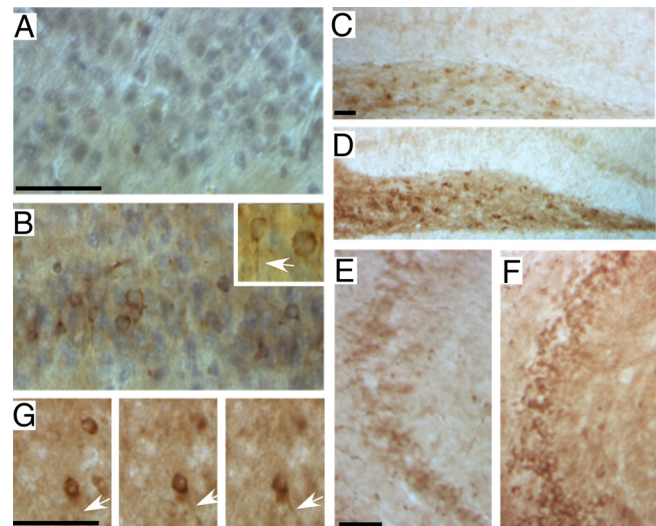


Fig. 2. Spatial distribution of phospho-tau in 4-month-old FeC γ 25 mice. Sagittal brain sections from 4-month-old non-transgenic wild-type mice (A, C, and E) or FeC γ 25 mice (B, D, and F) were stained with AT-8 antibody. A low basal level of staining, consistent with the Western blot data, is apparent in wild-type animals in entorhinal cortex (A), hilus of the dentate gyrus (C), and the CA3 region (E). The corresponding regions of FeC γ 25 mice (B, D, and F) show an increased amount of immunoreactivity. Phospho-tau is seen in the cell bodies and also axonal threads (arrow, inset in B). Panels in (G) show a section from FeC γ 25 mouse focused at different focal planes showing an axonal thread emanating from a cell body. (Scale bar, 25 μ m.)

4–6) displayed higher levels of sarcosyl-insoluble tau detected by phospho-tau antibodies (top three rows) or Tau5 antibody (bottom row) compared to wild-type mice (lanes 1–3). Thus, the AICD transgenic mice showed increased phosphorylation of tau beginning at 4 months of age, but tau aggregation became apparent only

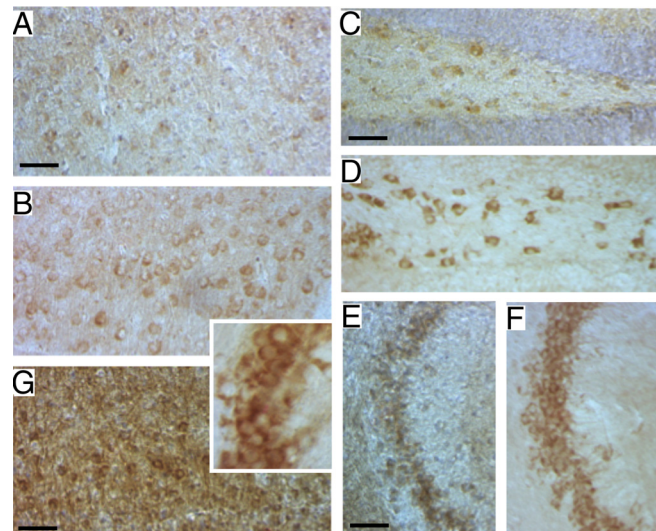


Fig. 3. Increased phospho-tau staining in 8-month-old FeC γ 25 mice. Sagittal brain sections from 8-month-old non-transgenic wild-type mice (A, C, and E) or FeC γ 25 mice (B, D, and F) were stained with AT-180 antibody. Similar to that observed at 4 months of age, the basal level of immunoreactivity is apparent in wild-type animals in entorhinal cortex (A), hilus of the dentate gyrus (C), and the CA3 region (E). Again, the corresponding regions of FeC γ 25 mice (B, D, and F) show an increased amount of immunoreactivity. There appears to be a greater accumulation of phospho-tau in the cell bodies of neurons in 8-month-old animals (inset in G from CA3 region). (G) Some FeC γ 25 mice show much higher levels of phospho-tau staining [compare with (B)]. (Scale bar, 25 μ m.)

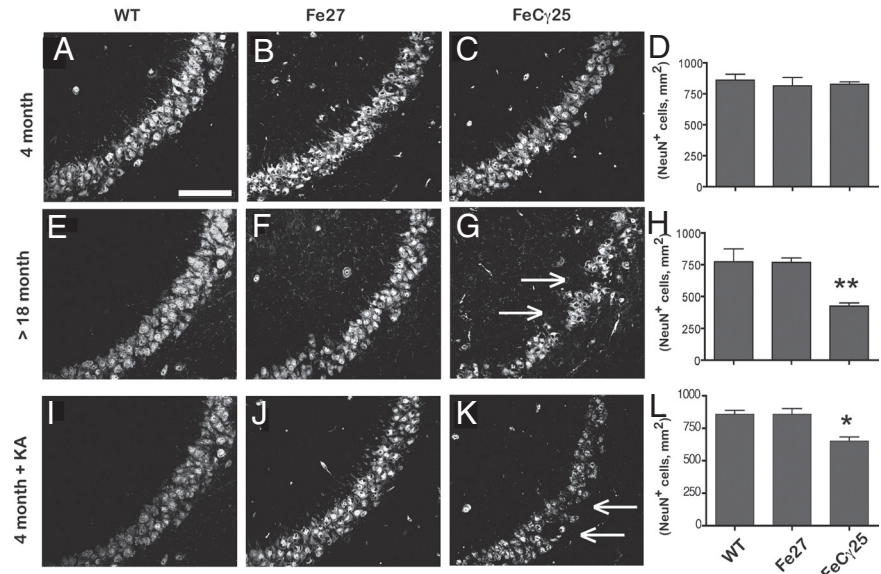


Fig. 4. FeCγ25 mice display an age-dependent loss of hippocampal neurons and increased sensitivity to excitotoxic stress. Sagittal sections from 4-month-old (top row) or >18 month-old (middle row) wild-type, Fe27, and FeCγ25 mice were stained with anti-NeuN antibody. (A–C) NeuN-positive cells from the CA3 region of the hippocampus. (D) Quantification shows an approximately equal number of neurons in wild-type and transgenic mice. (E–G) NeuN staining of area CA3 from >18-month-old mice. Arrows in g show the CA3 areas with neuronal loss in FeCγ25 mice. (H) Quantification of these data show an approximate 50% reduction in CA3 neurons in FeCγ25 mice compared to Fe27 mice or wild-type. (I–K) NeuN staining of area CA3 from 4-month-old mice 3 days after being injected with a subconvulsive dose of kainic acid. Arrows in (K) show the loss of neurons in CA3 regions of FeCγ25 mice. (L) Quantification of NeuN-positive cells shows neuronal loss in FeCγ25 mice after kainic acid treatment. * $P < 0.05$, ** $P = 0.01$, one way ANOVA (all data expressed as Mean \pm SEM). Arrows point to areas of neuronal cell loss, $n = 3$ for all groups. [Scale bar in (A), 100 μ m.]

at 7–8 months of age, indicating a lag period between tau hyperphosphorylation and aggregation.

We then performed immunohistochemistry on brain slices from 4-month-old mice (Fig. 2) to examine the phospho-tau distribution in brain. Consistent with the Western blot data, AT-8-positive immunostaining was elevated in the entorhinal cortex region of FeCγ25 mice (Fig. 2B) compared to the non-transgenic mice (Fig. 2A). AT-8 positive phospho-tau was observed both in the cell bodies and axonal threads (arrow in inset in Fig. 2B). FeCγ25 mice also showed increased phospho-tau staining in the Hilar region of the dentate gyrus (Fig. 2D) and the CA3 region of hippocampus (Fig. 2F) compared to the controls (Fig. 2C and E). The panels in Fig. 2G represent three focal planes of a section showing AT-8-positive axonal threads that originate from cell soma in FeCγ25 brain.

Increased levels of hyperphosphorylated tau were also seen in 8-month-old animals (Fig. 3) as well as 12-month-old animals (Fig. S2). Increased AT-180 immunoreactivity was observed in entorhinal cortex (Fig. 3B), Hilus of the dentate gyrus (Fig. 3D), and CA3 region of the hippocampus (Fig. 3F) in FeCγ25 mice compared to non-transgenic controls (Fig. 3A, C, and E). There was heterogeneity in the levels of phospho-tau staining, as some FeCγ25 animals showed a much higher staining intensity (Fig. 3G; similar heterogeneity was also observed with human AD samples, see Fig. 7A). By 8 months of age, the somatodendritic accumulation of phospho-tau was much more prominent (Fig. 3G, inset). We also observed increased phospho-tau immunoreactivity in FeCγ25 mice when stained with AT-8 antibody. Together, the immunohistochemical analyses show that phospho-tau levels are elevated in FeCγ25 mice compared to control mice.

FeCγ25 Mice Show Age-Dependent Neurodegeneration. Although neuronal loss is an invariable feature of AD brains, most mouse models of AD do not show neurodegeneration (24). To determine whether AICD expression induces the loss of hippocampal neurons, we killed mice at 4, 8, 12, and 18 months of age. Sagittal sections from wild-type, Fe27 and FeCγ25 mice were stained for the neuronal marker NeuN, and the NeuN-positive cells were counted in the dentate gyrus, CA1, and CA3 areas. There was no neuronal loss in 4-month-old mice area CA3 (Fig. 4 A–D) or any of the other hippocampal subfields among wild-type, Fe27, and FeCγ25 mice (Fig. S3). We also did not detect any significant changes in the number of neurons in the hippocampus of FeCγ25 mice at 8 or 12 months of age compared to age-matched control animals. However, in mice aged >18 months there was a significant loss of NeuN-

positive cells in the CA3 region of FeCγ25 mice compared to wild-type and Fe27 mice (Fig. 4 E–H, $P = 0.01$). We also observed neuronal loss to a lesser extent in the dentate gyrus but not in the CA1 region of aged FeCγ25 mice (Fig. S3).

The loss of neurons at >18 months of age but not at 4 months of age suggested that elevated levels of AICD might make the neurons susceptible to stressful insults accumulated throughout aging. To determine whether AICD increases neuronal vulnerability to toxic insults, we subjected mice to kainic acid-induced excitotoxic shock. When 4-month-old mice were administered a subconvulsive dose of kainic acid and examined 3 days later, we found a loss of CA3 neurons in FeCγ25 (Fig. 4 I–L, $P = 0.0074$) that resembled the loss in aged mice. However, there was no cell loss in area CA3 of wild-type mice (Fig. 4I) and Fe27 mice resembled the wild-type controls (Fig. 4J). Together, these data show that AICD transgenic mice show age-dependent neurodegeneration as observed in human AD. Also, the presence of AICD increases the susceptibility of neurons to external deleterious stimuli *in vivo*.

FeCγ25 Mice Exhibit Reduced Working Memory, Which Is Rescued by Lithium Treatment. Impaired memory is a neurological hallmark of AD, and a number of experimental paradigms have been developed to test various aspects of memory in animal models. We subjected animals to spontaneous alternation in the Y-maze paradigm, which has been used to detect working memory deficits in AD mice and in mice lacking NMDA receptor subunits (25) that learn normally in the water maze test. FeCγ25 mice assessed at 4 months of age did not exhibit any significant changes in spontaneous alternations (Fig. 5A) or total arms entered (Fig. 5B) when compared to wild-type or Fe27 mice. However, at 8 months of age, the FeCγ25 mice exhibited a statistically significantly decreased in spontaneous alternations compared to wild-type and Fe27 mice (Fig. 5C). These changes were not due to abnormal excitability, as the total arms entered were the same for all groups at 8 months of age (Fig. 5D). We also tested mice in the open field chamber at 4 and 8 months of age (Fig. S4) and observed no differences in their exploratory behavior. Thus, these data suggest that exploratory behavior remains intact, but working memory deteriorates at 8 months of age as phospho-tau starts to display increased insolubility.

Since FeCγ25 mice exhibited increased activity of the tau kinase GSK-3β (21), we next tested whether inhibition of GSK-3β activity rescues the working memory deficits seen in these mice. We put 7–8-month-old mice on a chronic diet of lithium in their chow (26). After 30 days on the diet, mice were assessed for spontaneous

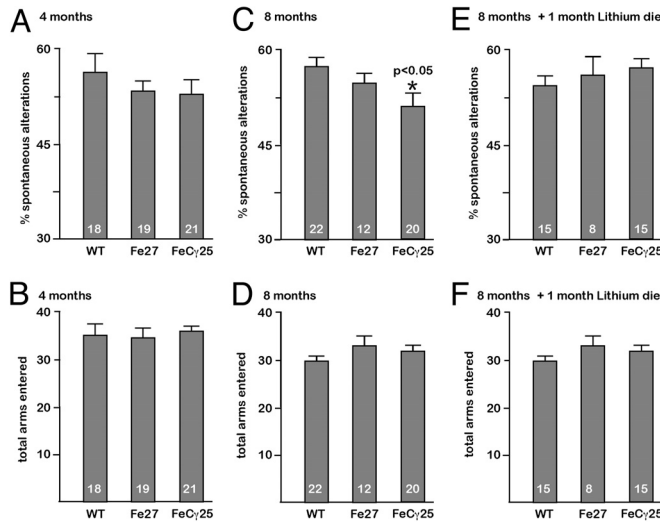


Fig. 5. Age-dependent deficits in working memory in FeC γ 25 mice. FeC γ 25 mice exhibit age-dependent deficits in working memory (*A*, *C*, and *E*) but not in exploratory behavior (*B*, *D*, and *F*) in the Y maze. The percentage of spontaneous alternations (working memory) for wild-type, Fe27 and FeC γ 25 mice at 4 months of age (*A*), 8 months of age (*C*), and 8 months of age after a 30-day lithium diet (*E*). Note that at 8 months of age, FeC γ 25 mice showed a small but significantly increased error rate compared to other animals. This deficit was largely abolished when age-matched animals were placed on lithium diet. The average number of arm entries (exploratory behavior) for wild-type, Fe27, and FeC γ 25 at 4 months of age (*B*), 8 months of age (*D*), and at 8 months of age after a 30-day lithium diet (*F*). There were no significant differences in any of the groups. The number at the bottom of each bar denotes the number of animals tested in each group. All data expressed as \pm SEM, * $P < 0.05$.

alternation in the Y-maze (at 8–9 months of age). We found that FeC γ 25 mice on the lithium diet performed much better and were indistinguishable from wild-type and Fe27 mice (Fig. 5*E*). We also did not detect any differences in the total arms entered (Fig. 5*F*), demonstrating no changes in exploratory activity while on the diet.

AICD Does Not Alter APP Processing or Increase A β Levels in Transgenic Mice. Most of the pathological features described above have also been observed in mouse models of AD, with accumulation of A β being implicated as the underlying cause. To determine if the deleterious events in AICD transgenic mice could be due to increased A β levels, we examined whether APP processing was altered in these mice. We found no significant changes in the levels of α -CTF (Fig. 6 *A* and *B*) or β -CTF (Fig. 6 *A* and *C*) in the hippocampus or cortex of wild-type versus FeC γ 25 mice. We could not reliably measure the brain A β levels, as determination of endogenous mouse A β is technically challenging. To circumvent this problem, we crossed FeC γ 25 with R1.40 transgenic mice, which produce higher levels of human A β by 1 month of age (27). We measured the levels of total A β by ELISA in 3–4-month-old mice and observed no significant differences between R1.40 and R1.40 \times FeC γ 25 mice (Fig. 6*D*). Finally, to determine if AICD could accelerate plaque formation, we crossed FeC γ 25 mice to APPPS1 transgenic mice which co-express APPswe and L166P mutant PS1 proteins (28). These mice overproduce A β 1–42 and exhibit A β deposition as early as 6–8 weeks of age. We examined A β -plaque load in 3–4-month-old APPPS1 and APPPS1 \times FeC γ 25 mice (Fig. 6*F*) and found no significant changes in plaque number (Fig. 6*E*) or plaque size. These data demonstrate that at the time we start to detect tau abnormalities in FeC γ 25 mice (3–4 months), increased levels of AICD do not cause gross alterations in APP processing or increased A β levels *in vivo*.

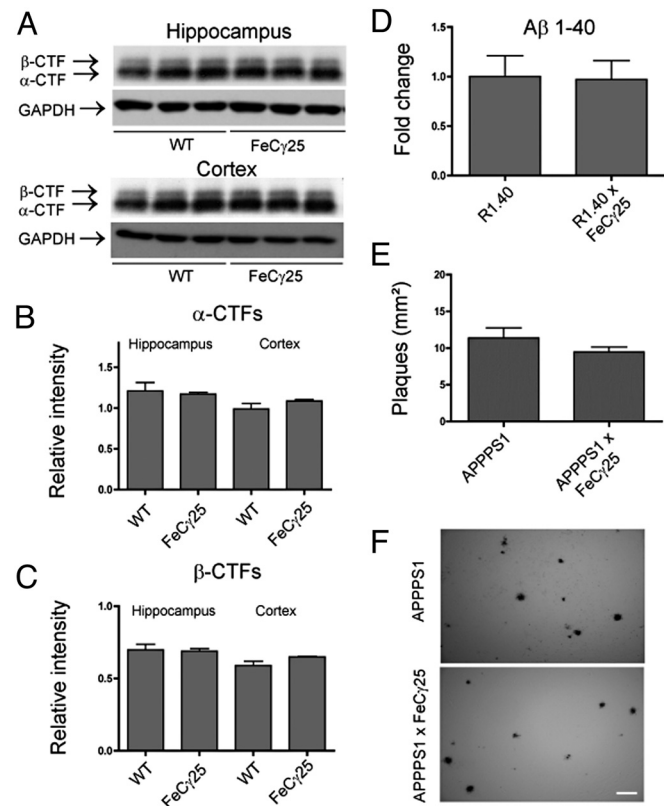


Fig. 6. AICD does not alter APP processing or increase A β levels. (*A*) Western blots from 3–4-month-old hippocampal and cortical lysates for APP carboxy-terminal fragments with APP anti-carboxy terminal 0443 antibody showing representative alpha and beta-cleaved bands and GAPDH loading controls. Each lane represents an individual mouse. (*B*) α -CTFs were quantified by normalizing the band intensity to that of GAPDH to determine the relative intensity for both hippocampal and cortical samples, with no significant differences in protein levels. (*C*) β -CTFs were quantified in the same manner as described for α -CTFs and show no significant differences in relative protein levels. (*D*) ELISA to detect A β 1–40 from 3–4-month-old hemi brains of R1.40 or R1.40 \times FeC γ 25 demonstrated no significant differences between groups. (*E*) 6E10-positive plaques were counted from 3–4-month-old APPPS1 or APPPS1 \times FeC γ 25 mice, with no apparent differences in the number of plaques. (*F*) Representative plaque deposition in APPPS1 and APPPS1 \times FeC γ 25 mice from cortices. All data expressed as mean \pm SEM, $n = 3$ for all groups. [Scale bar in (*F*), 100 μ m.]

AICD Levels Are Increased in Human AD Brains. Having demonstrated that AICD accumulation causes multiple AD-like features in mice, we next assessed the clinical relevance of these findings by examining AICD levels in human AD patients. Total protein extracts from 13 brain samples from confirmed AD patients and 12 samples from age matched non-demented controls were separated on 4–12% Novex gradient gels and blotted with 0443 antibody (that recognizes the C terminus of APP) as described previously (21). The top rows in Fig. 7*A* show the APP-CTF and AICD levels from AD brains and non-AD control brains. Although there was wide variation in AICD levels, they were significantly higher in AD samples compared to the non-AD samples. To ascertain equal loading, we stripped the blots and re-probed with antibodies to GAPDH (middle rows). AICD levels were quantified by measuring band pixel density using the NIH ImageJ software and normalized for the amount of GAPDH loaded. Quantification of these data (Fig. 7*B*) showed that despite variation, AICD levels were significantly higher in AD brains than in control brains ($P = 0.0002$). We also probed these samples for phospho-tau levels using AT-8 antibody (lower rows) and observed generally higher levels of

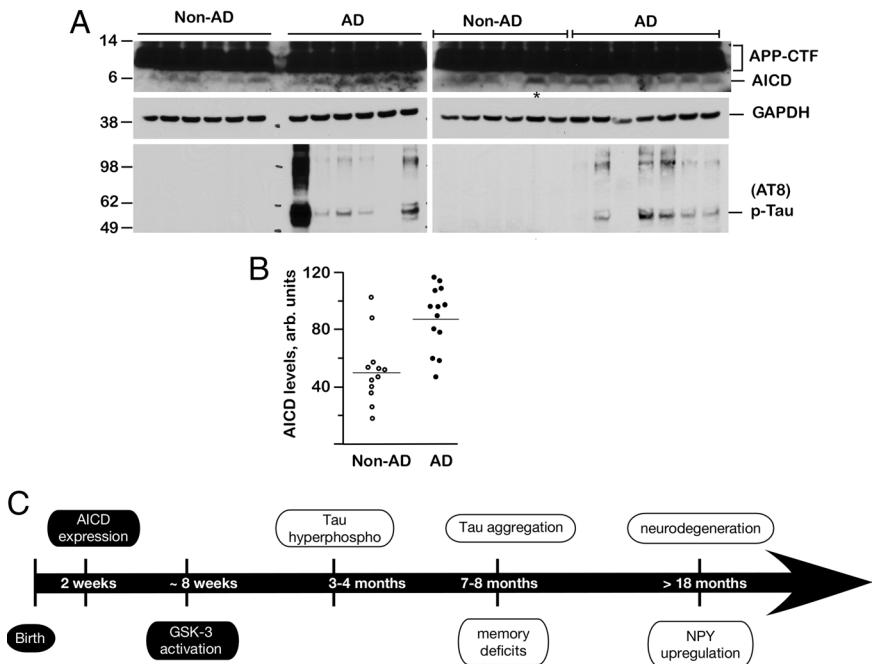


Fig. 7. AICD levels are increased in human AD brains. (A) Brain lysates from 13 AD patients (AD) and 12 non-dementia control subjects (Non-AD) were analyzed by SDS/PAGE and Western blotted with 0443 antibody (top rows) that recognizes APP-C terminus or AT-8 antibody (bottom rows). Blots were stripped and reprobed with GAPDH (middle rows). The upper rows show APP-CTF and AICD levels, which were quantified by NIH ImageJ software (B). Although there was a large variation in the AICD levels, they were significantly elevated in AD patients compared to non-demented controls ($P = 0.0017$). The lane marked with * in A (right panel) marks the non-AD sample with abnormally high AICD levels (an outlier). The wide variation in AD samples is also seen in phospho-tau levels. (C) Summary of pathological events observed in FeCy25 mice. AICD expression is driven by a CaMKII α promoter, which becomes active around P15, and activation of GSK-3 β is observed at 6–8 weeks. Increased phosphorylation of tau is first observed at 3–4 months of age, although tau does not become aggregated until 7–8 months of age. Memory deficits become first apparent at this time point. Neuronal loss and up-regulation of NPY are not observed up to 12–15 months of age but become apparent >18 months of age. AD-related pathological features described in this study are shown in open ovals.

phospho-tau and aggregated-tau in AD brains with a considerable degree of variation (Fig. 7A). Interestingly, phospho-tau was not detected in any of the 12 non-demented control samples. Thus, these data show that AICD levels are elevated in human AD brains.

Discussion

Multiple lines of investigation suggest that $A\beta$ peptides play a central role in AD pathogenesis, and yet many results remain discordant with the amyloid hypothesis. Attempts to reconcile this discordance have led to the proposal that non- $A\beta$ factors also contribute to AD pathology (11, 12). Generation of $A\beta$ peptides is obligatorily coupled to that of AICD; both result from the cleavage by presenilin and the loss of presenilin gene function abolishes the production of both (16). Pathological effects of $A\beta$ have been described in various transgenic mouse models, but similar information for AICD has been lacking. The present studies demonstrate that AICD transgenic mice exhibit features of AD in an age-dependent manner. These mice show activation of GSK-3 β at 1–2 months of age (21), increased phosphorylation of tau at 3–4 months of age and tau aggregation at 7–8 months of age. Deficits in working memory are first observed by 7–8 months of age and loss of hippocampal neurons is seen in mice older than 18 months. Such histological, neurological and neurodegenerative changes are also found in human AD brains (29) and attributed to accumulation of $A\beta$. However, 4-month-old AICD transgenic mice show normal APP metabolism, normal $A\beta$ levels and do not accelerate $A\beta$ deposition when crossed to other mouse models of AD. Thus, these data indicate that in addition to $A\beta$, overexpression of AICD in vivo causes pathological features of AD in animal models. Future studies will be needed to determine the individual contribution of each peptide to AD pathogenesis.

Based on the evidence presented here, we propose that increased levels of AICD initiate a series of events that begins with activation of GSK-3 β at 1–2 months of age and culminates in neurodegeneration at 18 months of age (Fig. 7C). CaMKII α promoter that drives the expression of AICD/Fe65 transgenes becomes active at P15, and it is possible that other unidentified events precede GSK-3 β activation and contribute to downstream effects. Nonetheless, the observation that chronic treatment with lithium-blocked working memory deficits indicates that activation of GSK-3 β is one of the more prominent deleterious effects of AICD

overexpression. Aberrant activation of GSK-3 β is considered to be one of the key pathological feature of AD (22). The cumulative observations that AICD activates GSK-3 β in vitro (20) and in vivo (21), AICD levels are elevated in human AD brains (this study), and that inhibition of GSK-3 β protects against tau phosphorylation (30), neurodegeneration (31), and memory deficits provide a strong evidentiary framework for an $A\beta$ -independent pathological pathway. Such a scenario also provides a reasonable explanation for observations such as the poor correlation between $A\beta$ load and degree of disease severity or the disappointing results from $A\beta$ -centered clinical trials without contradicting the basic tenet of the amyloid hypothesis.

The AICD transgenic mice display age-dependent neurodegeneration, an invariant feature of AD that is not recapitulated in most mouse models (such as Tg2576). It is likely that in addition to GSK-3 β activation, AICD also regulates other events that are relevant to AD pathogenesis (32). Interestingly, a mutation in the AICD portion of APP (D664A) decreases its transcriptional activity (33) and blocks memory deficits in a transgenic mouse model of AD, which nonetheless maintain high levels of $A\beta$ (9). The underlying basis of the effect of D664A mutation is unclear (it has been implicated in caspase cleavage of APP), but at a minimum these reports are consistent with our assertion that AICD contributes to AD-like features.

Despite the evidence that AICD plays a significant role in AD pathology, our data do not imply that AICD is the primary pathogenic agent and the demonstration that AICD causes deleterious effects does not negate the data that show the harmful effects of $A\beta$. Indeed, it is possible that AICD may act synergistically with $A\beta$ in potentiating the disease [however, our preliminary observations indicate that AICD transgenic mice lacking $A\beta$ (generated by crossing FeCy25 mice with APP-KO mice) also recapitulate many pathological features]. Also, FAD mutations in APP have been shown to increase the $A\beta$ levels or alter the $A\beta$ 42:40 ratio without affecting AICD levels (34). However, one caveat of such studies is that AICD was generated in tissue culture cells using an in vitro assay, which may not faithfully replicate what happens in vivo. At present, there are no known systematic studies that address whether FAD mutations in APP and presenilin cause increased production of AICD in vivo. Our preliminary data in R1.40 and APPswe transgenic mice (expressing APPswe and APPswe+PS1L166P,

respectively) indicate elevated levels of AICD in the brains. However, it is uncertain whether the increased AICD levels in these mice are due to the mutations per se or due to increased levels of APP transgene. Future studies are needed to carefully examine whether and which of the FAD mutations in APP or presenilin cause increased production of AICD in vivo.

Finally, the finding that AICD levels are elevated in human AD brains provides support for the clinical relevance of the data presented here. We currently do not know why AICD accumulates in AD brains. One possibility is that AICD, like APP-CTFs (35), is degraded by proteasomes in tissue culture cells and deficient proteasomal degradation has been implicated in AD (36). Uncovering the mechanisms underlying AICD accumulation or its downstream signaling events will be important as it may offer targets for therapeutic intervention.

In summary, the present study shows that increased levels of AICD in vivo are capable of producing pathological features of AD. One aspect of our findings is that AICD exerts these effects apparently in an $\text{A}\beta$ -independent manner. We propose that the pathological features observed in AD mouse models arise from AICD as well as $\text{A}\beta$. If these implications can be further validated in humans, an important prediction of the present study will be that eliminating the toxic effects of $\text{A}\beta$ alone will be insufficient to abolish all pathological features of AD.

Methods

Mice. The generation and characterization of FeC₂₅ transgenic mice (co-expressing AICD and Fe65) or Fe27 transgenic mice (expressing Fe65 alone) have

been previously described (21). R1.40 and APPPS1 mice have been described elsewhere (27, 28). Lithium diet was prepared by adding lithium carbonate (2.4 g/kg) to animal food and purchased from Bio-Serve, Inc.. All experiments were approved by the IACUC of The Cleveland Clinic.

Tissue Preparation and Immunostaining. Hemi-brains were fixed overnight in 4% paraformaldehyde in PBS, sunk in 30% sucrose and embedded in OCT. Thirty-micrometer sagittal sections were cut and every 12th section was used. Antibodies used were NeuN (Chemicon, 1:800) and NPY (Immunostar, 1:1,000), AT-8 (Pierce, 1:500), and AT-180 (Pierce, 1:250). Remaining details are given in the *SI Text*.

Western Blots. Hippocampal and cortical tissue was isolated from mice at 3–4 months of age and homogenized in tissue lysis buffer. Membranes were incubated in primary antibodies (AT-8, AT-180, PHF1, and Tau5, all at 1:1,000 dilution) overnight at 4 °C. Primary antibodies used were anti-APP C-terminal antibody 0443 (Calbiochem, 1:2,000) and GAPDH (Chemicon, 1:40,000). Antigen retrieval technique was used while detecting human AICD (21). ImageJ was used for densitometric analysis, and bands were normalized to GAPDH loading controls for each sample.

Behavioral Analysis. Equal numbers of male and female mice were tested by placing them in the center of a Y-shaped maze (21 cm length × 8.5 cm width × 40 cm height) and being allowed to freely explore for 5 min. The testing surface was sterilized with ethanol between each trial.

Rest of the protocols are described in the *SI Text*.

ACKNOWLEDGMENTS. We thank Dustin Thomas for maintaining the mouse colony and Chris Nelson for his comments on the manuscript. This work was supported by a National Institutes of Health Grant R01AG026146, Alzheimer's Association, and CART-Rotary Funds (to S.W.P.) and National Institutes of Health Training Grant T32 HD007104 (to D.L.V.).

1. Hardy J, Duff K, Hardy KG, Perez-Tur J, Hutton M (1998) Genetic dissection of Alzheimer's disease and related dementias: Amyloid and its relationship to tau. *Nat Neurosci* 1:355–358.
2. Price DL, Sisodia SS (1998) Mutant genes in familial Alzheimer's disease and transgenic models. *Ann Rev Neurosci* 21:479–505.
3. Zheng H, Koo EH (2006) The amyloid precursor protein: Beyond amyloid. *Mol Neurodegener* 1:5.
4. Selkoe DJ (1998) The cell biology of beta-amyloid precursor protein and presenilin in Alzheimer's disease. *Trends Cell Biol* 8:447–453.
5. Hardy J, Selkoe DJ (2002) The amyloid hypothesis of Alzheimer's disease: Progress and problems on the road to therapeutics. *Science* 297:353–356.
6. Price DL, Tanzi RE, Borcetti DR, Sisodia SS (1998) Alzheimer's disease: Genetic studies and transgenic models. *Ann Rev Genet* 32:461–493.
7. Holmes C, et al. (2008) Long-term effects of $\text{A}\beta$ 42 immunotherapy in Alzheimer's disease: Follow-up of a randomized, placebo-controlled phase I trial. *Lancet* 372:216–223.
8. Scheff SW, Price DA (2003) Synaptic pathology in Alzheimer's disease: A review of ultrastructural studies. *Neurobiol Aging* 24:1029–1046.
9. Galvan V, et al. (2006) Reversal of Alzheimer's-like pathology and behavior in human APP transgenic mice by mutation of Asp664. *Proc Natl Acad Sci USA* 103:7130–7135.
10. Simon AM, et al. (2008) Overexpression of wild-type human APP in mice causes cognitive deficits and pathological features unrelated to $\text{A}\beta$ levels. *Neurobiol Dis* 33:369–378.
11. Small SA, Duff K (2008) Linking $\text{A}\beta$ and tau in late-onset Alzheimer's disease: A dual pathway hypothesis. *Neuron* 60:534–542.
12. Pimplikar SW (2009) Reassessing the amyloid cascade hypothesis of Alzheimer's disease. *Int J Biochem Cell Biol* 41:1261–1268.
13. Haass C, Selkoe DJ (2007) Soluble protein oligomers in neurodegeneration: Lessons from the Alzheimer's amyloid beta-peptide. *Nat Rev Mol Cell Biol* 8:101–112.
14. Townsend M, Shankar GM, Mehta T, Walsh DM, Selkoe DJ (2006) Effects of secreted oligomers of amyloid beta-protein on hippocampal synaptic plasticity: A potent role for trimers. *J Physiol* 572:477–492.
15. Lesne S, et al. (2006) A specific amyloid-beta protein assembly in the brain impairs memory. *Nature* 440:352–357.
16. De Strooper B, et al. (1998) Deficiency of presenilin-1 inhibits the normal cleavage of amyloid precursor protein. *Nature* 391:387–390.
17. Gao Y, Pimplikar SW (2001) The gamma-secretase-cleaved C-terminal fragment of amyloid precursor protein mediates signaling to the nucleus. *Proc Natl Acad Sci USA* 98:14979–14984.
18. Cao X, Südhof TC (2001) A transcriptionally [correction of transcriptionally] active complex of APP with Fe65 and histone acetyltransferase Tip60. *Science* 293:115–120.
19. Muller T, et al. (2007) Modulation of gene expression and cytoskeletal dynamics by the amyloid precursor protein intracellular domain (AICD). *Mol Biol Cell* 18:201–210.
20. von Rotz RC, et al. (2004) The APP intracellular domain forms nuclear multiprotein complexes and regulates the transcription of its own precursor. *J Cell Sci* 117:4435–4448.
21. Ryan KA, Pimplikar SW (2005) Activation of GSK-3 and phosphorylation of CRMP2 in transgenic mice expressing APP intracellular domain. *J Cell Biol* 171:327–335.
22. Hooper C, Killick R, Lovestone S (2008) The GSK3 hypothesis of Alzheimer's disease. *J Neurochem* 104:1433–1439.
23. Andorfer C, et al. (2003) Hyperphosphorylation and aggregation of tau in mice expressing normal human tau isoforms. *J Neurochem* 86:582–590.
24. Schmitz C, et al. (2004) Hippocampal neuron loss exceeds amyloid plaque load in a transgenic mouse model of Alzheimer's disease. *Am J Pathol* 164:1495–1502.
25. Bannerman DM, et al. (2008) NMDA receptor subunit NR2A is required for rapidly acquired spatial working memory but not incremental spatial reference memory. *J Neurosci* 28:3623–3630.
26. Nocjar C, Hammonds MD, Shim SS (2007) Chronic lithium treatment magnifies learning in rats. *Neuroscience* 150:774–788.
27. Lehman EJ, Kulnane LS, Lamb BT (2003) Alterations in beta-amyloid production and deposition in brain regions of two transgenic models. *Neurobiol Aging* 24:645–653.
28. Radde R, et al. (2006) $\text{A}\beta$ 42-driven cerebral amyloidosis in transgenic mice reveals early and robust pathology. *EMBO Rep* 7:940–946.
29. Brunovsky M, Matousek M, Edman A, Cervena K, Krajca V (2003) Objective assessment of the degree of dementia by means of EEG. *Neuropsychobiology* 48:19–26.
30. Plattner F, Angelo M, Giese KP (2006) The roles of cyclin-dependent kinase 5 and glycogen synthase kinase 3 in tau hyperphosphorylation. *J Biol Chem* 281:25457–25465.
31. Huang HC, Klein PS (2006) Multiple roles for glycogen synthase kinase-3 as a drug target in Alzheimer's disease. *Curr Drug Targets* 7:1389–1397.
32. Liu Q, et al. (2007) Amyloid precursor protein regulates brain apolipoprotein E and cholesterol metabolism through lipoprotein receptor LRP1. *Neuron* 56:66–78.
33. Zambrano N, et al. (2004) Fe65 is not involved in the platelet-derived growth factor-induced processing of Alzheimer's amyloid precursor protein, which activates its caspase-directed cleavage. *J Biol Chem* 279:16161–16169.
34. Hecimovic S, et al. (2004) Mutations in APP have independent effects on $\text{A}\beta$ and CTF γ generation. *Neurobiol Dis* 17:205–218.
35. Nunan J, et al. (2001) The C-terminal fragment of the Alzheimer's disease amyloid protein precursor is degraded by a proteasome-dependent mechanism distinct from gamma-secretase. *Eur J Biochem* 268:5329–5336.
36. Oddo S (2008) The ubiquitin-proteasome system in Alzheimer's disease. *J Cell Mol Med* 12:363–373.